Electronic Supplementary Information (ESI) for

Structural Discrimination of Double-Walled Carbon Nanotubes by Chiral Diporphyrin Nanocalipers

Gang Liu,[a] Yukie Saito,[b] Daisuke Nishio-Hamane,[c] Ajoy K. Bauri,[d] Emmanuel Flahaut,[e] Takahide Kimura[a] and Naoki Komatsu*[a]

[a] *Department of Chemistry, Shiga University of Medical Science, Seta, Otsu 520-2192, Japan. Fax: 81-77-548-2405; Tel: 81-77-548-2102; E-mail: nkomatsu@belle.shiga-med.ac.jp*

[b] *Graduate School of Agricultural and Life Sciences, The University of Tokyo, 1-1-1 Yayoi, Bunkyo-ku, Tokyo, 113-8657, Japan*

[c] *The Institute for Solid State Physics, The University of Tokyo, 5-1-5 Kashiwanoha, Kashiwa, Chiba, 277-8581, Japan*

[d] *Bio-Organic Division, Bhabha Atomic Research Center, Trombay, Mumbai, 400085, India*

[e] *Université de Toulouse; UPS, INP, CNRS; Institut Carnot Cirimat; 118, route de Narbonne, F-31062 Toulouse cedex 9, France.*

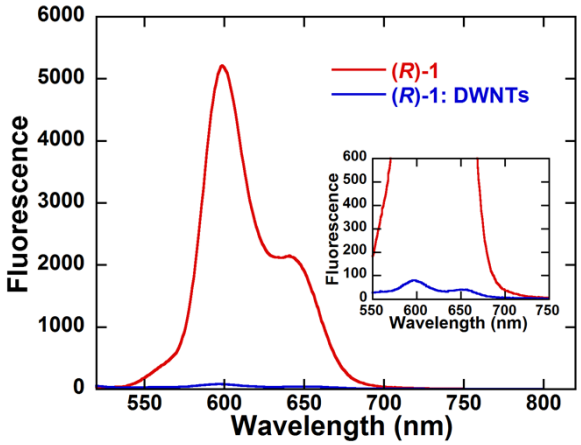

Figure S1. Fluorescence spectra of (*R*)-**1** in methanol before and after the extraction of DWNTs. The (*R*)-**1** and the DWNT extract were excited at 419 nm and 440 nm, respectively.

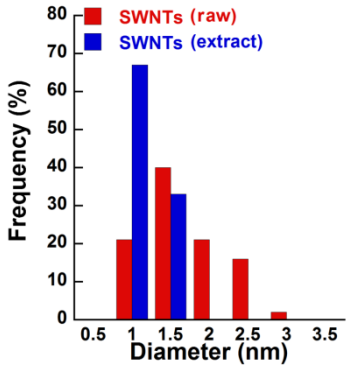

Figure S2. Diameter distribution of SWNTs before and after the extraction with nanocalipers **1**. The histogram is prepared with a diameter steps of 0.5 nm.

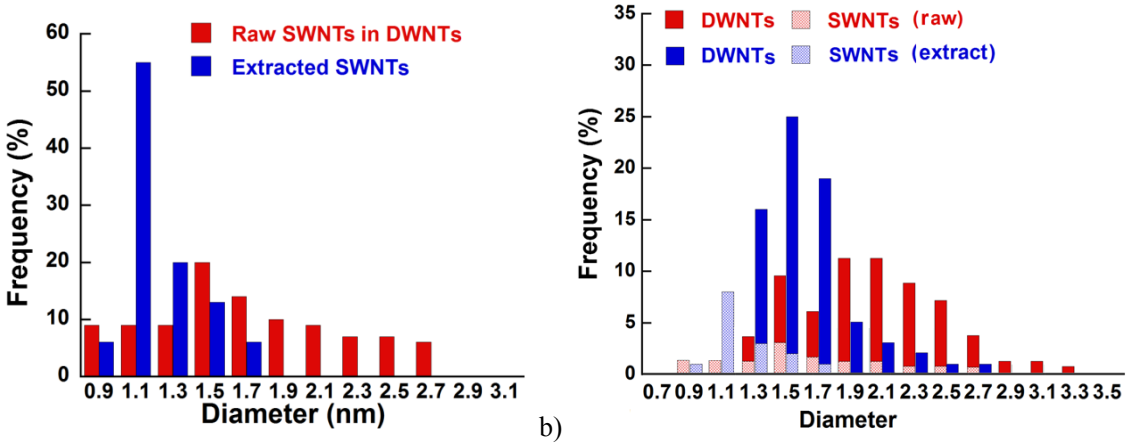

a) b)

Figure S3. Diameter distribution of SWNTs (a) and CNTs (SWNTs + DWNTs) (b) before and after the extraction with nanocalipers **1**. The histograms are prepared with a diameter steps of 0.2 nm. The distribution in diameter of raw sample is adapted from the reference; T. Hertel, A. Hagen, V. Talalaev, K. Arnold, F. Hennrich, M. Kappes, S. Rosenthal, J. McBride, H. Ulbricht, E. Flahaut, *Nano. Lett*., **2005**, *5*, 511-514.

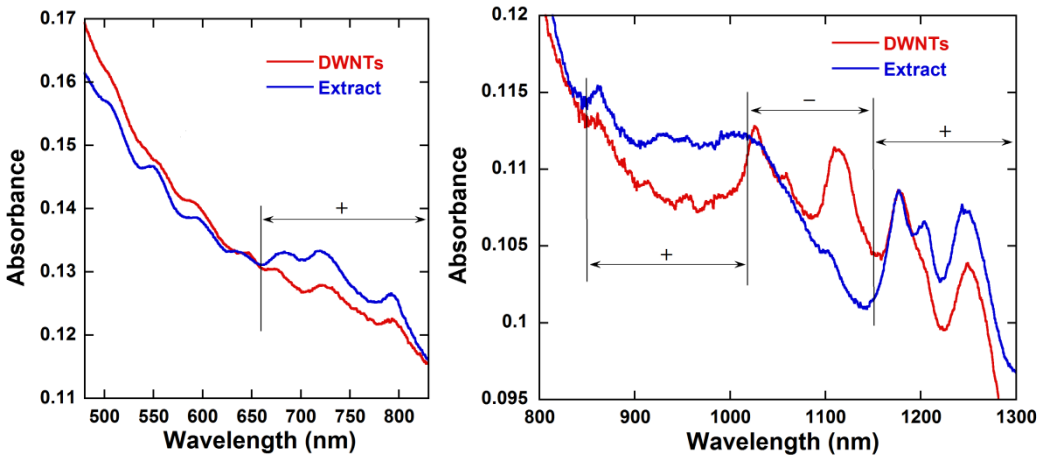

Figure S4. Absorption spectra of DWNTs before and after the extraction with (*R*)-**1**.

Possible interpretation in absorption spectra of the extract for diameter selectivity

The SDBS-D_2O dispersion of the washed CNTs was analyzed with absorption spectroscopy to further confirm the diameter selectivity. Although the observed bands are not so sharp as those of SWNTs used in our studies (ref. 28, 31 and 32 in the main text), spectral change is observed clearly through extraction with nanocalipers **1** as shown in Figure S4.

While the peaks in the region of 1020 – 1150 nm significantly decrease in intensity, the increase in peak intensity is observed at the regions of 650 – 800 nm, 860 – 1020 nm, and 1140 – 1280 nm, which are translated to the energy and diameter ranges as summarized in Table S1, based on the Kataura plot (ref. 1 in the main text).

Table S1. Diameter range of CNTs increasing in the absorption intensity after the extraction.

Range [nm] in absorption increase	Corresponding energy range [eV]	Corresponding diameter range [nm] (optical transition)
650 - 800	1.6 – 1.9	0.9 - 1.0 (E^S_{22}) 1.3 - 1.6 (E^M_{22}) > 1.6 (E^S_{33})
860 – 1020	1.2 – 1.4	1.1 – 1.4 (E^S_{22}) > 1.7 (E^M_{22})
1140 – 1280	1.0 – 1.1	0.7 – 0.8 (E^S_{11}) 1.5 – 1.6 (E^S_{22})

The absorption range of 650 – 800 nm can be attributed to the semiconducting tubes with the diameter ranges of 0.9 – 1.0 nm and > 1.6 nm, and the metallic tube with 1.3 – 1.6 nm (Table S1). In the absorption range, the peak intensity in the higher energy band around 700 nm (1.8 eV) increase more significantly, indicating that relatively small diameters in each diameter range enriched more than larger ones. Since metallic tubes are less abundant than semiconducting ones statistically, it can be said that the DWNTs with a pair of inner and outer tubes having ~0.9 nm and ~1.6 nm in diameters, respectively, enriched through the extraction. This is consistent with the enriched inner and outer diameters of DWNTs determined by HR-TEM as shown in Figures 4b and 4c in the main text. The next absorption range is 860 – 1020 nm corresponding to the semiconducting tube with the diameter range of 1.1 – 1.4 nm and the metallic tube

with > 1.7 nm (Table S1). Focusing on the semiconducting rather than the metallic at the same reason as that mentioned above, the enriched diameter range of 1.1 – 1.4 nm in Table S1 is consistent with that of 1.09 – 1.48 nm in Table 1 (in the main text) determined by Raman spectra excited at 488 nm. As for the absorption range of 1140 – 1280 nm, the corresponding tubes with 0.7 – 0.8 nm and 1.5 – 1.6 nm in diameters can be considered as a pair of inner and outer tubes in DWNTs as in the case of the absorption range of 650 – 800 nm. The diameter ranges for enriched inner and outer tubes are included in those determined by HR-TEM shown in Figure 4b and 4c in the main text.

Experimental section

Materials: DWNTs were prepared by catalytic chemical vapour deposition (CCVD) as reported previously (ref. 14 in the main text). All the reagents were obtained from Sigma-Aldrich Co., Wako Pure Chemical Industries, Ltd., Nacalai Tesque, Inc., and Tokyo Chemical Industry Co., Ltd. and were used as received unless otherwise noted. The chiral porphyrin and its derivatives were synthesized according to the reported procedures (ref. 32 in the main text).

Equipment: UV-vis-NIR absorption spectra were obtained on a UV-3100PC scanning spectrophotometer (Shimadzu Co.). Fluorescence spectra were performed on a F-4500 spectrophotometer (Hitachi Co.). Raman spectra were measured on LabRam HR800 (Horiba Ltd.), and take the average of more than ten different spots for the final curve. Circular dichroism spectra were recorded on J-820 spectropolarimeter (JASCO International Co. Ltd). ^{1}H NMR (270 MHz) and ^{13}C NMR (67.5 MHz) measurements were conducted on a JEOL JNM-EX-270 spectrometer. Centrifugation was carried out with Avanti J-E and Optima-TL (Beckman Coulter, Inc). Tip-sonication was performed with MISONIX (138 W, 20 kHz). SEM and STEM were carried out on a JEOL JSM-7500F field emission scanning electron microscope, operating at 25 kV accelerating voltage for SEM and TEM model, respectively. HR-TEM was conducted using a JEOL JEM-2100 transmission electron microscope at an accelerating voltage of 200 kV.

Calculation: The calculations in molecular modeling were carried out by use of the MMFF molecular mechanics in the Spartan ’08 (Version 1.2.0).

Synthesis of 2,7-bis(9-octyl-9H-carbazol-3-yl)pyrene: The mixture of 3-bromo-9-octyl-9*H*-carbazole (1.13 g, 3.15 mmol), 2,7-bis(4,4,5,5-tetramethyl-1,3,2-dioxaborolan-2-yl)pyrene (311 mg, 0.69 mmol), $Pd(PPh_3)_4$ (36 mg, 0.030 mmol), and Cs_2CO_3 (2.04 g, 6.26 mmol) in dry DMF (10 ml) and dry toluene (20 ml) was deoxygenated for 15 min, and then stirred at 90 °C for 12 h under Ar. After adding another portion of 2,7-

bis(4,4,5,5-tetramethyl-1,3,2-dioxaborolan-2-yl)pyrene (311 mg, 0.69 mmol) and stirring for 12 h, the reaction mixture was poured into water and extracted with dichloromethane. The combined organic layers were dried over anhydrous $MgSO_4$, filtered, and concentrated under vacuum. The residue was purified by column chromatography. Yield: 62%. ^{1}H NMR (270 MHz, $CDCl_3$, δ): 8.61 (d, J = 1.6 Hz, 2H; Cz H), 8.53 (s, 4H; Py H), 8.25 (d, J = 7.8 Hz, 2H; Cz H), 8.19 (s, 4H; Py H), 8.02 (dd, J_1 = 8.6 Hz, J_2 = 1.6 Hz, 2H; Cz H), 7.45-7.59 (m, 6H; Cz H), 7.26-7.33 (m, 2H; Cz H), 4.37 (t, J = 7.3 Hz, 4H; CH_2), 1.89-2.01 (m, 4H; CH_2), 1.26-1.45 (m, 20H; CH_2), 0.88 (t, J = 6.8 Hz, 6H; CH_3).

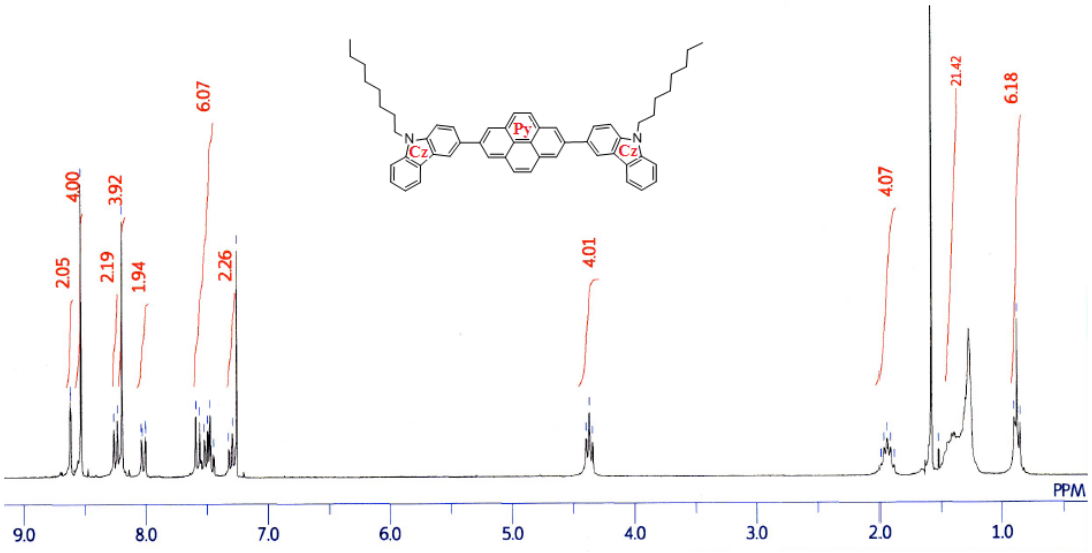

Synthesis of 2,7-bis(6-bromo-9-octyl-9H-carbazol-3-yl)pyrene: *N*-Bromosuccinimide (135 mg, 0.76 mmol) was added slowly to a solution of 2,7-bis(9-octyl-9*H*-carbazol-3-yl)pyrene (280 mg, 0.37 mmol) in dichloromethane (150 ml) at 0 °C. After stirring for 3 h, the mixture was concentrated, and the residue was purified by column chromatography. Yield: 71%. ^{1}H NMR (270 MHz, $CDCl_3$, δ): 8.54 (d, J = 1.6 Hz, 2H; Cz H), 8.49 (s, 4H; Py H), 8.34 (d, J = 1.8 Hz, 2H; Cz H), 8.18 (s, 4H; Py H), 8.03 (dd, J_1 = 8.6 Hz, J_2 = 1.6 Hz, 2H; Cz H), 7.54-7.61 (m, 4H; Cz H), 7.29-7.34 (m, 2H; Cz H), 4.33 (t, J = 7.3 Hz, 4H; CH_2), 1.86-1.99 (m, 4H; CH_2), 1.24-1.41 (m, 20H; CH_2), 0.88 (t, J = 6.8 Hz, 6H; CH_3).

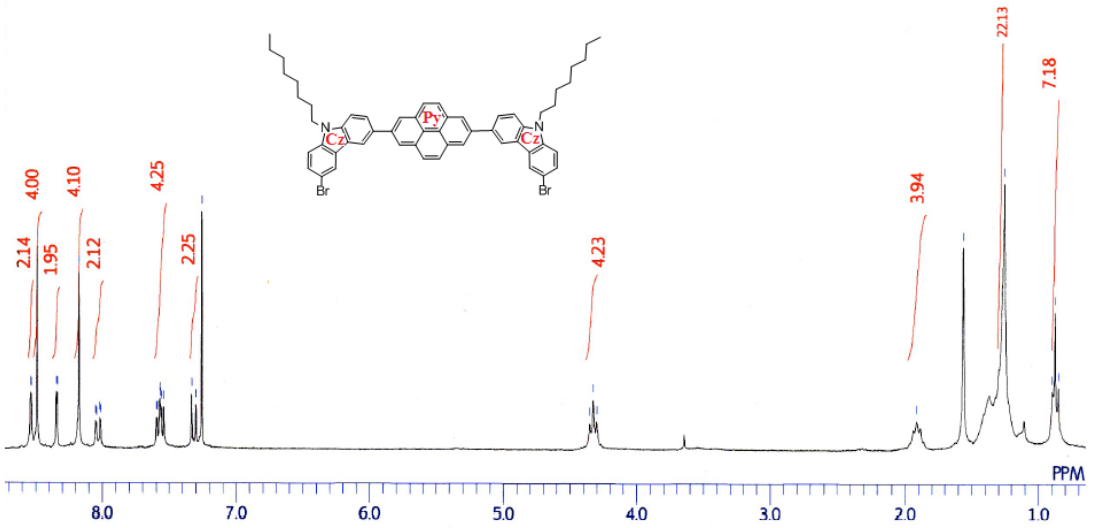

Synthesis of Chiral Diporphyrin (R)-**1**: 2,7-Bis(6-bromo-9-octyl-9H-carbazol-3-yl)pyrene (12 mg, 0.013 mmol), 5-(4′,4′,5′,5′-tetramethyl-[1′,3′,2′]dioxaborolan-2′-yl)-10,20-di(1″-*tert*-butoxycarbonyl-amino- 2″-phenylethyl)-(*R*)-porphinatozinc(II) (19 mg, 0.031 mmol), Cs_2CO_3 (30 mg, 0.093 mmol), and $Pd(PPh_3)_4$ (3.4 mg, 0.0030 mmol) were dissolved in a mixture of dry DMF (3.0 ml) and dry toluene (3.0 ml). After deoxygenation, the mixture was stirred at 85 °C for 8 h under Ar. After the addition of water, the product was extracted with dichloromethane. The extract was dried over anhydrous $MgSO_4$, passed through a short silica gel column, and concentrated. The residue was subjected to recycling preparative GPC-HPLC to give chiral diporphyrin nanocalipers (*R*)-**1** as purple solid. Yield: 43%. UV-vis (MeOH): λ_{max}: 419, 554, and 591 nm. Fluorescence (MeOH, λ_{ex} = 419 nm); λ_{max} = 599 and 641 nm.

Since decent spectra of NMR and ESI-MS of the zinc diporphyrin were not obtained, the corresponding free base diporphyrin was prepared by acid-treatment of the zinc diporphyrin and subjected to ^{1}H NMR analyses. ^{1}H NMR (270 MHz, $CDCl_3$, δ, Figure S5): 10.08 (s, 2H; P H), 9.44-9.51 (m, 8H; P H), 9.28-9.33 (m, 4H; P-H), 8.92-9.01 (m, 6H; P-H, Cz H), 8.67 (s, 2H; Cz H), 8.46 (s, 4H; Py H), 8.26 (d, *J* = 9.0 Hz, 2H; Cz H), 8.11 (d, *J* = 9.0 Hz, 2H; Cz H) 8.03 (s, 4H; Py H), 7.75 (d, *J* = 9.6 Hz, 4H; Cz H), 7.32-7.41 (m, 4H; B H), 6.90-7.01 (m, 16H; B H), 6.22 (s, 4H; CH), 4.57-4.69 (m, 4H; CH_2), 4.21-4.39 (m, 8H; CH_2), 2.12-2.24 (m, 4H; CH_2), 1.22-1.45 (m, 56H; CH_2, CH_3), 0.86-0.99 (m, 10H; CH_3, NH), -2.80 (s, 4H; NH); ^{13}C NMR (67.5 MHz, $CDCl_3$, δ, Figure S6): 14.15, 22.70, 27.58, 28.34 (br), 29.33, 29.55, 29.88, 31.90, 43.74, 48.74, 58.13, 79.88, 104.54, 106.49, 109.53, 117.46 (br), 120.15, 121.46, 121.53, 123.39, 123.58, 123.89, 126.31, 126.48, 127.77, 128.23, 129.29, 131.45, 132.72 (br), 132.95, 133.81, 138.59, 139.52, 140.63, 141.01, 146.62 (br), 155.41. ESI-MS *m*/*z* (Figure S4): $[M + 2H]^{2+}$ calcd for $C_{148}H_{150}N_{14}O_{82}^{2+}$, 1126.0891; found, 1126.0897.

The chiral diporphyrin (*S*)-**1** was synthesized from 5-(4′,4′,5′,5′-Tetramethyl-[1′,3′,2′] dioxaborolan-2′-yl)-10,20-di(1″-*tert*-butoxycarbonyl-amino-2″-phenylethyl)-(*S*)-porphinatozinc(II) according to the procedure described for (*R*)-**1**.

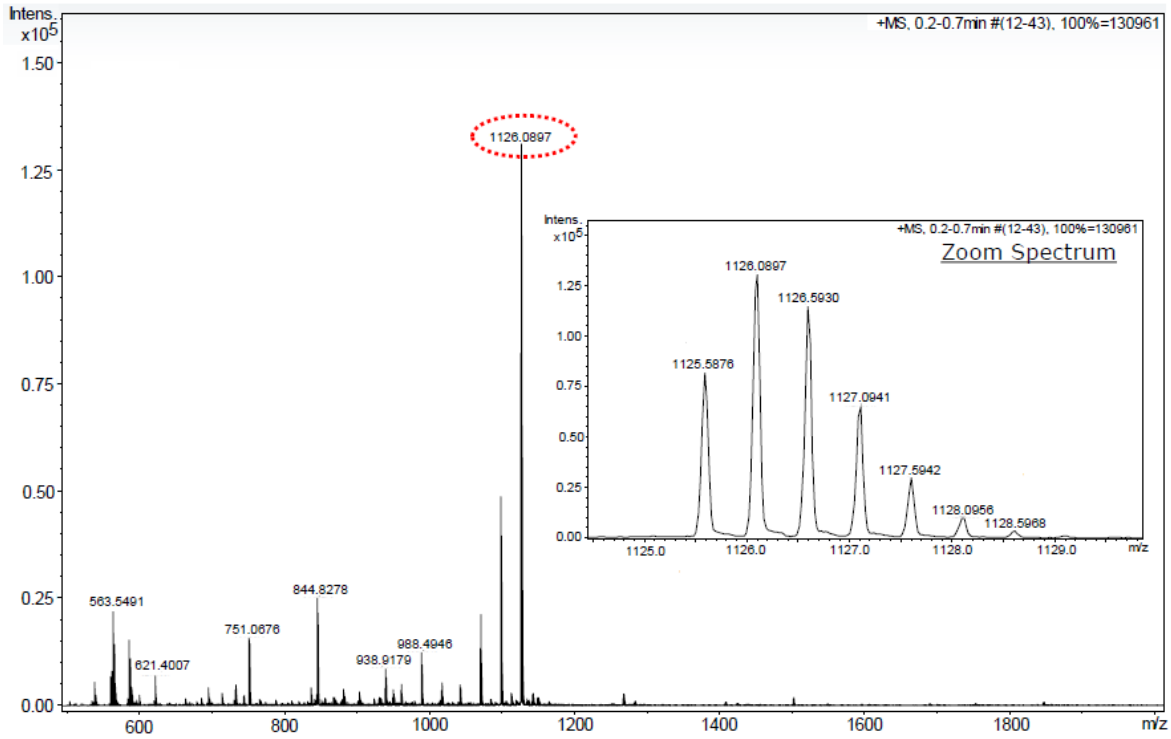

Figure S5. ESI-MS spectrum of free base diporphyrin after removal of the Zn in (*R*)-**1**.

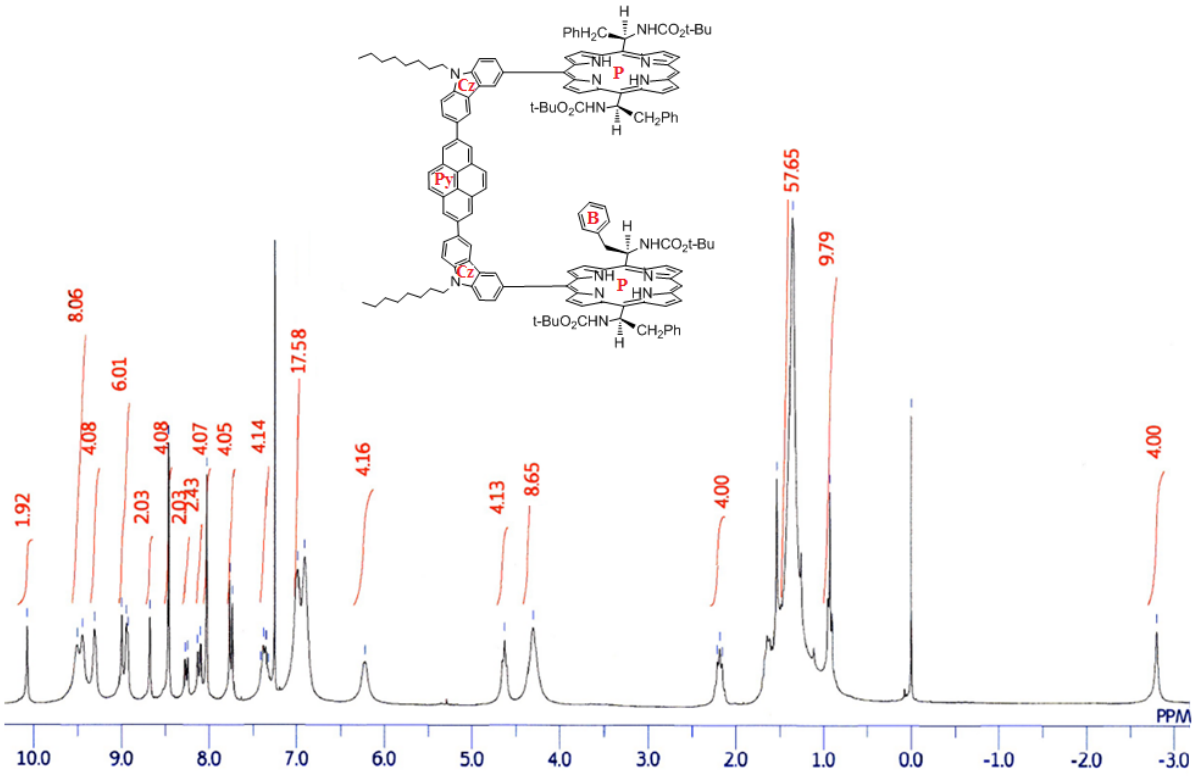

Figure S6. [1]H NMR spectrum of free base diporphyrin after removal of the Zn in (*R*)-**1**.

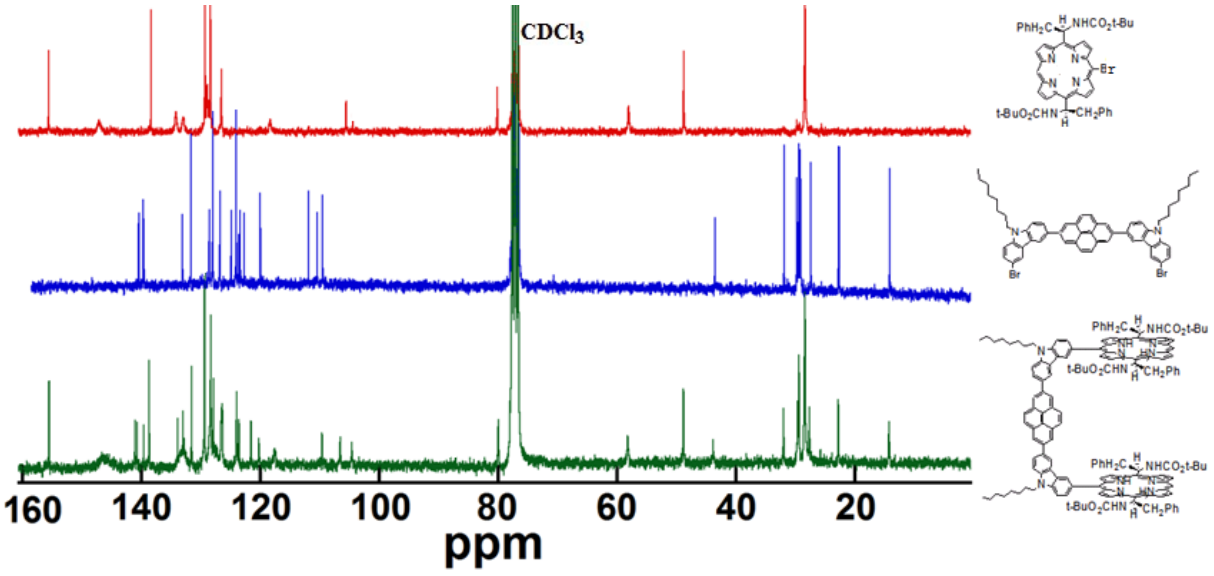

Figure S7. [13]C NMR spectra of free base monoporphyrin, spacer, and free base diporphyrin after removal of Zn in (*R*)-**1**.